MRI/PET insert: investigations of eddy currents on copper shields in the bore

B. J. Peng[1], J. Walton[2], C. Catana[1], S. R. Cherry[1], and J. Willig-Onwuachi[1,3]

[1]BMEGG, Biomedical Engineering, University of California, Davis, CA, United States, [2]NMR Facility, University of California, Davis, CA, United States, [3]Physics, Grinnell College, Grinnell, IA, United States

Abstract: A PET insert for simultaneous PET and MR imaging is being developed [1]. The PET electronics are enclosed in a shield located a minimum axial distance of 77mm from the magnet iso-center [1]. In this abstract we examine the induction of eddy currents on a simplified model of the PET shield. First, we use a CSI technique to investigate the effects of eddy currents using our current geometry. Second we explore alternate shield concepts for reduction of eddy current related artifacts if the shield is moved closer to the imaging volume.

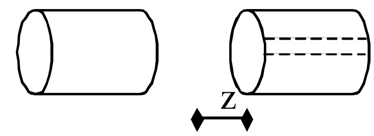

Fig. 1 Shield geometry. Z is axial distance from iso-center. Dashed lines indicate direcion of breaks, if breaks present.

Introduction: The insert was designed for use in the bore of a 7T 120mm bore MR scanner and utilizes a short length of optical fiber from scintillation crystals to avalanche photodiodes (APDs) used for light detection. All of the PET electronics are housed in a metal shield. Selecting the axial location for the PET electronics is a trade off between better PET performance (shorter optical path length) and better MRI performance (shield and electronics farther from the imaging volume). In earlier studies, eddy current effects were minimal when the shield was located beyond a 5cm axial distance from the iso-center [2]. To test this we used a chemical shift imaging (CSI) technique. Eddy currents perturb the B_0 field changing the resonant frequency or chemical shift (in ppm). Because eddy currents are induced by fast switching gradients and die off with time, lengthening the echo time should decrease the effects of eddy currents resulting from the slice select or inserted test gradients. Also presented below is an initial analysis of how adjusting the shield thickness and slitting the shield can reduce eddy currents and thus might enable moving the electronics closer to iso-center.

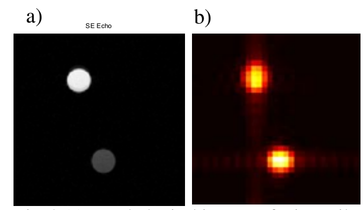

Fig. 2 (a) morphological images of crisco oil (top) and water (bottom). (b) maximum magnitude images from reconstructing CSI pixel data.

Methods: The interaction between the PET shield and the MR system is dominated by the inner copper cylinder closest to the RF coil and imaging volume. For all experiments presented, we use a simplified model of the PET shield consisting of two copper cylinder elements 65mm in diameter (representing the inner shield) and 115mm in axial length placed symmetrically about iso-center (Fig. 1). For the CSI experiments the shields were 50.8µm (0.002") thick, placed at z=5cm, and supported by a carbon fiber tube. The phantom consisted of one thin tube filled with water and another filled with Crisco oil. The resonance frequency of Crisco oil does not vary significantly with temperature. We used a CSI2D (SE) pulse sequence with TR=1000ms, TE=9,10,…30ms, matrix size 16x16 zero-filled to 32x32, and spectral dimension 2048. We compared chemical shift data with the shields to data without the shield and without the carbon fiber support tube. For our CSI analysis, we selected the pixel with the highest intensity in the oil phantom from the short-TE image. For the other experiments we made five different copper shields with the same radial and axial dimensions. Shields A, B, and E have a single 50.8µm (0.002"), 76.2µm (0.003"), and 25.5µm (0.001") thick layer respectively. Shield C consists of two 25.4 µm (0.001") layers separated by a layer of regular printer paper—one continuous layer and one with 1cm gaps running axially (Fig. 1). Shield D has a single 0.002" layer with 1cm gaps running axially. A plastic tube was used to support the RF coil (inside) and shields (around the outside). For each shield we acquired phantom images with axial shield location, z, ranging from 0-12cm in 2cm increments and a reference image with the shield moved out of the bore. SE (TR=1000ms, TE=11.6ms) and GE (TR=500ms, TE=4.1ms, 30^0 tip) data were collected (slice thickness=1mm, Nslice=8, 128x128 matrix) and normalized root mean square error (NRMSE) was calculated and plotted [2].

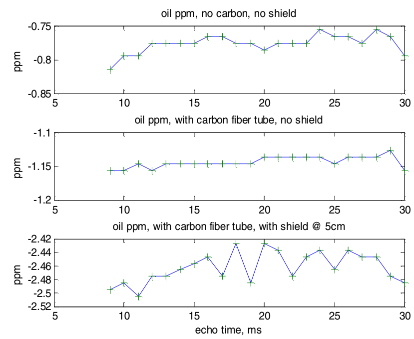

Fig 3. Oil ppm vs. Echo Time (ms)

Results and Discussions: Fig. 3 shows chemical shift versus TE for (a) no additional materials, (b) only the carbon fiber tube, and (c) the shield with support tube present. None show a trend with increasing TE, leading us to believe that we are not detecting any significant eddy currents. Refinements of this experiment are currently being planned to verify this result. We note that the observed variation is loosely correlated to the quality of the shim achieved in each case (9.8, 4.9, and 18.5 Hz for a-c), but we are not aware of any reason to expect this. Introduction of the shield indeed makes it more difficult to achieve a good shim because of susceptibility differences between the copper and air. Fig. 4 shows plots of NMRSE vs. shield location for a GE sequence. SE results were similar. Note that for the solid shields (E, A, & B), errors generally increase at all shield locations for increased copper thickness, as expected. Note also that those shields with breaks had reduced errors for the z=0 location compared to our current shield (A), because the breaks interrupt the current path around the circumference of the cylinder. Being able to place the shield right at iso-center opens the possibility of reducing the length of or eliminating altogether the fiber optic cables between the scintillation crystals and the APD detectors. For shields C and D with breaks, artifacts were noticeably absent from images (and subtraction images). Representative GE images with and without eddy current artifacts are shown in Fig. 5. The double layer design C is similar to D and E but could provide more stable shielding. The continuous cylinder can act as a DC ground for the electronics, while the gapped layer provides additional RF shielding below the GHz range. Note that this is only a preliminary exploration of the shield design's impact on MR image quality. We have not validated the level of RF shielding using these shields. However, the actual shield uses a double-sided solid Cu cladding with 0.35µm thickness, for which measured noise leakage is small and no RF interference has been observed in MR images. Alternative methods of introducing shield breaks while maintaining the necessary PET shielding still must be examined. We are optimistic, however that the shield can be moved to z=0 with other designs.

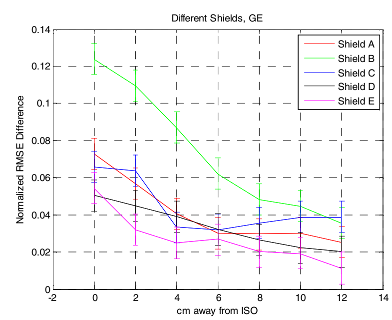

Fig. 4 Five different shields and their GE plots of normalized RMS error difference vs. distance.

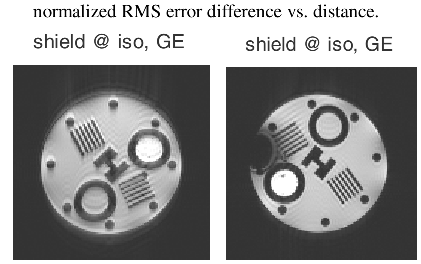

Fig. 5 Representative GE images with eddy current artifacts (left, Shield B) and without (right, Shield C).

Reference: [1] C. Catana, Y. Wu, M.S. Judenhofer, J. Walton, B.J. Peng, J. Willig-Onwuachi, B.J. Pichler and S.R. Cherry, "Combining PET and MRI – Challenges in Developing an MR Compatible PET insert," #785, ISMRM 2006. [2] B. J. Peng, C. Catana, J. Walton2, S. R. Cherry, J. Willig-Onwuachi, "Placing a PET insert in the bore of a 7T magnet: Initial study of the interactions of the MRI system with the PET shielding," #1358, ISMRM 2006.